Peer-reviewed version available at *Catalysts* **2018**, *8*, 380; doi:10.3390/catal8090380

Article

High Active and Selective Ni/Ceo$_2$-Al$_2$O$_3$ and Pd-Ni/Ceo$_2$-Al$_2$O$_3$ Catalysts for Oxy-Steam Reforming of Methanol

Pawel Mierczynski*[1], Agnieszka Mierczynska[2], Radoslaw Ciesielski, Magdalena Mosinska[1], Magdalena Nowosielska[1], Agnieszka Czylkowska[1], Waldemar Maniukiewicz[1], Malgorzata I. Szynkowska[1], Krasimir Vasilev[3]

[1] Institute of General and Ecological Chemistry, Lodz University of Technology, Zeromskiego 116, 90 - 924 Lodz, Poland; e-mail@e-mail.com

[2] The Australian Wine Research Institute, Waite Precinct, Hartley Grove cnr Paratoo Road, Urrbrae (Adelaide) SA 5064

[3] Mawson Institute, University of South Australia, Mawson Lakes SA 5095, Adelaide, Australia

* Correspondence: pawel.mierczynski@p.lodz.pl, tel. + 48 42 631 31 24, Fax: 0048 42 631 31 28

Agnieszka Mierczynska: agnieszka.mierczynsaka-vasilev@awri.com.au

Radoslaw Ciesielski: radoslaw.ciesielski@p.lodz.pl

Magdalena Mosinska: m.mosinska@op.pl

Magdalena Nowosielska: magdalena.nowosielska@p.lodz.pl

Agnieszka Czylkowska: agnieszka.czylkowska@p.lodz.pl

Waldemar Maniukiewicz: waldemar.maniukiewicz@p.lodz.pl

Malgorzata I. Szynkowska:malgorzata.szynkowska@p.lodz.pl

Krasimir Vasilev: krasimir.vasilev@unisa.edu.au

Abstract: Herein, we report about the monometallic Ni and bimetallic Pd-Ni catalysts supported on CeO$_2$-Al$_2$O$_3$ binary oxide, which were investigated in oxy-steam reforming of methanol (OSRM). Monometallic and bimetallic supported catalysts were prepared by wet aqueous impregnation and subsequent impregnation method, respectively. The physicochemical properties of the catalytic systems were investigated using various methods such as: BET, XRD, TPR-H$_2$, TPD-NH$_3$, XPS and SEM-EDS techniques. It has been proven that the addition of palladium to the nickel catalyst facilitates its reduction. The activity tests performed for all catalysts confirmed the promotion effect of palladium on catalytic activity of nickel catalyst and selectivity towards hydrogen production. Both nickel and bimetallic palladium-nickel supported catalysts showed excellent stability during the reaction. Such catalytic systems are valuable for the advance of the field of fuel cell technology.

Keywords:OSRM; nickel; bimetallic catalyst; heterogeneous catalysis; Pd-Ni

1. Introduction

Over the last decades there have been substantial efforts to develop environmentally friendly sources of energy, capable of replacing fossil fuels [1-3]. One of the sources that have captured attention is hydrogen since it combust without the release of pollutants easy [4-10]. The increased interest in hydrogen is associated with the use of hydrogen to power fuel cells [11, 12]. On the other hand, the fuels cell technology and hydrogen can replace currently dominant fossil fuels. Therefore, research related to the development of fuel cells may lead to the commercialization of fuel cell technology.

Preprints (www.preprints.org) | NOT PEER-REVIEWED | Posted: 2 August 2018 doi:10.20944/preprints201808.0050.v1

Peer-reviewed version available at Catalysts 2018, 8, 380; doi:10.3390/catal8090380

Hydrogen can be produced by decomposition of methanol and via steam or oxygen reforming of methanol. These reactions can be coupled in a single process called oxy-steam reforming of methanol [1, 6, 13-16]. This is very advantageous from economics point of view because the process itself extends in an auto-thermal way without the need to provide external heat to carry out the reaction. Catalysts are essential to run mentioned processes with high yield and selectivity common catalysts used during these processes are copper and nickel based systems supported on mono and binary oxides [5, 14, 17-24].

Typically, in reforming of methanol reactions, both mono and binary oxide supports [8, 10, 13, 19, 21, 25-30] are used. To improve the catalytic activity, stability and selectivity different modifiers are added to the catalytic systems. Type of support and its nature as well as a preparation method has a great influence on the Ni based catalyst activity and stability.

Information about the usage of CeO_2 as modifiers of the Ni based catalysts is available in the literature. It was found that the introduction of cerium (IV) oxide into nickel based catalysts improves the metallic dispersion, limits agglomeration of the particles and enhances the metal-support interaction. All of these factors had a positive effect on the catalytic activity of nickel supported catalysts in dry reforming of methane [31]. Li et al. [32] studied CeO_2-promoted Ni/Al_2O_3-ZrO_2 catalyst in methane reforming with CO_2 reaction. They have found that addition of CeO_2 into monometallic nickel effectively improves the dispersion of Ni particles on the catalyst surface and enhances the stability of the nickel catalyst. The authors have also reported about an increased CO_2 adsorption on the catalyst surface after the introduction of CeO_2. Ahmed et al. [33] investigated the effect of ceria on the catalytic activity of Ni/CeO_2-Al_2O_3 systems in thermo-catalytic decomposition of methane. The results confirmed that ceria itself has great influence on the catalytic activity and stability. It was also proven that CeO_2 influence on the size of the Ni particle and the catalyst morphology. The reducibility results confirmed that promotion of Ni/Al_2O_3 catalyst by CeO_2 inhibits the nickel aluminate formation. The promotion of copper catalyst by CeO_2 also leads to an increase the thermal stability [34]. In addition cerium (IV) oxide can provide mobile oxygen which has direct influence on the catalytic activity and may affects on the valance state of the metal present on the support surface under reducing environmental

An attractive route for CeO_2-Al_2O_3 synthesis is co-precipitation method [35]. The binary oxide prepared by this method allow to obtain better dispersion of the active species on its surface compared to the catalysts supported on bi-oxide carrier prepared by impregnation method [36]. The activity results performed over Ni catalysts supported on monoxide CeO_2 and Al_2O_3 and binary oxide CeO_2-Al_2O_3 in methane thermo-catalytic decomposition shows that Ni/CeO_2-Al_2O_3 systems showed better catalytic properties compared to the mono-oxides [33]. It was also proven that the CeO_2 content [33] and the treatment conditions of the synthesized carrier CeO_2-Al_2O_3 have great influence on their catalytic and physicochemical properties. It is well documented in literature data that the preparation method of the support has a large impact on its physical and chemical properties [37, 38]. The selection of the appreciate preparation method of binary oxide influence on the interaction between the support and active phase component. All this has substantial influence on the catalytic properties of the catalytic material.

It is also well known in the literature data that promotion of monometallic catalysts by precious metals in most cases improves the catalyst activity [13], stability and selectivity in methanol reforming processes. The addition of precious metals to monometallic catalysts facilitates their reduction and affects their acidic and electron properties. Palladium is active component for methanol reforming reactions. It is an effective decomposition catalyst, selectively forming H_2 and CO when it is supported on metal oxide [39-41]. However, when palladium is supported on ZnO, high selectivity for CO_2 in the SRM reaction has been reported. This change in selectivity can be explained by the Pd-Zn alloys formation[42]. These palladium alloys form at moderate temperatures under reducing conditions[43].

2. Results and Discussion

2.1. Catalytic performance in oxy-steam reforming of methanol

The catalytic activity tests in oxy-steam reforming of methanol were performed at two temperatures 200 and 250 °C, respectively. The results of the activity are expressed as methanol conversion and selectivity towards all products and are given in Table1. The activity results showed that conversion of methanol increases with increase of the metal content. The highest methanol conversion among all tested nickel catalysts showed 40%Ni/CeO_2-Al_2O_3 system which exhibited also the highest hydrogen yield at 250 °C. A further increase in the nickel content caused a decrease in catalytic activity. The reactivity results confirmed also the promotion effect of palladium on the methanol conversion of nickel catalyst at both temperatures of the reaction. In addition, palladium enhanced the selectivity of the nickel catalyst towards hydrogen formation (see Table 1). To better understand the influence of the support composition on the catalytic activity in OSRM analogous tests were performed on nickel catalysts supported on Al_2O_3 or CeO_2 monoxides containing the same nickel content. The activity results are given in the same Table 1. The results indicate the higher activity of 40%Ni/CeO_2 compared to 40%Ni/Al_2O_3 but lower than the analogous catalyst supported on binary oxide. It is worth noticing that Ni catalyst supported on CeO_2 exhibited higher methanol conversion (85%) and high selectivity to hydrogen at 250 °C compared to Ni/Al_2O_3 catalyst. In comparison, Ni/Al_2O_3 catalyst showed low methanol conversion (20.5%) at 250°C, and formation of carbon monoxide during the reaction was not observed.

Table 1. Effect of temperature on the catalytic activity and selectivity to hydrogen, carbon monoxide, carbon dioxide, DME in the oxy-steam reforming of methanol over monometallic Ni catalysts supported on Al_2O_3, CeO_2, CeO_2-Al_2O_3 and bimetallic Pd-Ni catalysts supported on binary oxide CeO_2-Al_2O_3.Reaction condition: weight of catalyst = 0.2 g, $H_2O/CH_3OH/O_2$ molar ratio in the reaction mixture = 1/1/0.4, temperature of the reaction 200 and 250°C. The catalytic tests were performed under atmospheric pressure (GHSV = 26700 h^{-1}).

Catalyst	**CH_3OH conv. [%]**		**H_2 Selectivity [%]**		**CO Selectivity [%]**		**CO_2 Selectivity [%]**		**DME Selectivity [%]**	
	200 °C	**250° C**	**200° C**	**250° C**	**200° C**	**250° C**	**200° C**	**250° C**	**200° C**	**250° C**
5%Ni/CeO_2-Al_2O_3	-	2	-	30.5	-	-	-	25	-	44.5
20%Ni/CeO_2-Al_2O_3	11	31	66.5	33	-	-	26.3	55.6	7.2	11.4
40%Ni/CeO_2-Al_2O_3	40	98	45.2	68.9	46	13.3	8.3	14.3	0.5	3.5
60%Ni/CeO_2-Al_2O_3	18	77	61.4	58.2	-	27.7	38.6	14.1	-	trace
40%Ni/CeO_2	4	85	75	68.6	24.2	22.6	-	0.5	0.8	8.3
40%Ni/Al_2O_3	-	20.5	-	53.4	-	-	-	25.2	-	21.4
2%Pd-40%Ni/CeO_2-Al_2O_3	67	99.9	70.3	71.5	21.8	14.9	7.6	9.1	0.3	4.5

Peer-reviewed version available at Catalysts 2018, 8, 380; doi:10.3390/catal8090380

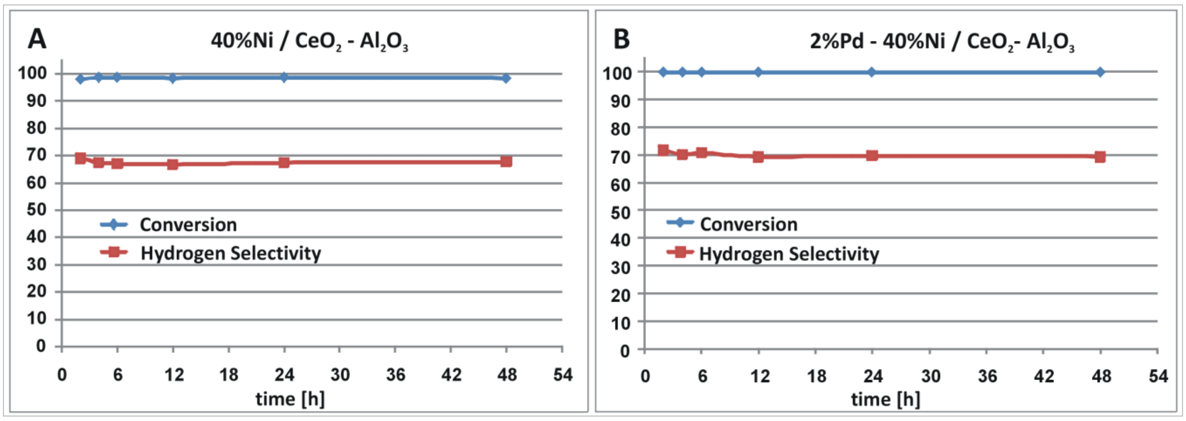

Figure 1. Methanol conversion and selectivity towards hydrogen formation for A) monometallic Ni/CeO_2-Al_2O_3 supported catalyst and B) bimetallic Pd-Ni/CeO_2-Al_2O_3 during 48 h of the reaction performed at 250 °C after reduction 1h at 300 °C in a mixture of 5%H_2-95%Ar.). Reaction condition: weight of catalyst = 0.2 g, H_2O/CH_3OH/O_2 molar ratio in the reaction mixture = 1/1/0.4, temperature of the reaction 200 and 250°C. The catalytic tests were performed under atmospheric pressure (GHSV = 26700 h^{-1}).

Pérez-Hernández et al. [22] investigated the catalytic properties of monometallic nickel, copper and bimetallic Cu-Ni catalysts supported on ZrO_2 in oxy-steam reforming of methanol reaction. They tested nickel catalyst with low Ni loading (about 2.44 % wt. of Ni) in OSRM process in the temperature range 250-300 °C (GHVS = 30 000 h^{-1}) and obtained the lowest conversion of methanol value below 14 % and the lowest selectivity towards hydrogen production. While all investigated catalysts showed comparable selectivity towards H_2 at the maximum reaction temperature (about 60%). It is also worth mentioning that nickel supported catalysts showed high CO selectivity. The total methanol conversion was obtained for the Ni/ZrO_2 catalyst at a temperature of 350 °C. This, results agree well with our activity results. We detected also only 2% of methanol conversion at 250 °C for 5%Ni/CeO_2-Al_2O_3 system. Similar reactivity results are shown in work [14]. Authors tested also monometallic 3% Cu/ZrO_2, 3% Ni/ZrO_2 and bimetallic Ni-Cu systems in OSRM (GHVS = 24 000 h^{-1}) in the temperature range 200-350 °C and confirmed the lowest activity of Ni catalyst in the studied temperature range. At 350 °C nickel catalyst showed below 70% of methanol conversion in the investigated process. The selectivity towards CO production at 350°C was about 10% for the monometallic Ni and Cu catalysts and about 40% for the bimetallic supported catalysts. Whereas, the results of the selectivity towards hydrogen production, showed that bimetallic catalysts exhibited high hydrogen yield close to the theoretical value. However, monometallic systems showed about 60 % of the hydrogen yield in the OSRM reaction.

In the next step of our reactivity results we tested the stability of both monometallic nickel and bimetallic Pd-Ni catalysts in oxy-steam reforming of methanol. The results of the stability tests in OSRM reaction on monometallic nickel and bimetallic Pd-Ni catalysts supported on CeO_2-Al_2O_3 within 48 h are presented in Figure 1. Both mono and bimetallic catalysts exhibited high and stable activity and selectivity towards hydrogen production at the investigated temperature. Both mono and bimetallic catalysts exhibit stable performance over the 48 hours of reaction as shown in Figure 1. López et al. [14] investigated the stability of the bimetallic Cu-Ni/ZrO_2 catalysts in oxy-steam reforming process within 50 hours on stream at a temperature of 300 °C. They monitored also the methanol conversion and selectivity towards hydrogen production values. The stability tests performed within 50 hours on stream showed high stability of the catalyst. The methanol conversion was stable and equal about 85%. While, the selectivity towards hydrogen was low and reached the value around 43%. Our catalytic systems showed markedly higher activity and selectivity towards hydrogen production. The stability tests showed that both monometallic and bimetallic catalysts exhibited high activity equal about 100% and the selectivity towards hydrogen formation around

70%. These activity and stability tests confirmed that the prepared catalysts may be potentially applied in fuel cell technology to produce hydrogen used to power them.

2.2. Specific surface area and chemisorption measurements

The specific surface area (SSA) measurements were performed for all catalytic systems and the results were given in Table 2. The SSA results showed that the highest specific surface area had alumina oxide. On the other hand cerium (IV) oxide was characterized by the lowest specific surface area of 60 m^2/g. CeO_2-Al_2O_3 system had intermediate value of specific surface area. The addition of nickel oxide into catalytic support causes the decrease of the specific surface area value of the support. This is due to the blockage of the support pores by metal oxide phase which is an active phase component of the catalyst. An analogous behaviour was observed for nickel supported catalytic systems after palladium addition. In the case of the monolayer capacity results the same trend was observed. The addition of the active phase component results in a decrease of the monolayer capacity values independently on the catalyst support used. The results are in agreement with those of monometallic nickel supported catalysts [33].

Table 2. BET surface area, monolayer capacity and dispersion degree of metallic nickel phase of supports and supported nickel catalysts calcined in air atmosphere for 4h at 400 °C.

Catalytic material	BET surface area [m^2/g]	Monolayer capacity [cm^3/g]	Metal Dispersion [%]	Metal area [m^2g^{-1} of Metal]	Crystallite size [nm]	H_2 sorption [$\mu molH_2gcat^{-1}$]	X^a [%]
Al_2O_3	210	48.2	-	-	-	-	-
CeO_2	60	13.8	-	-	-	-	-
CeO_2-Al_2O_3	145	33.2	-	-	-	-	-
5%Ni/CeO_2-Al_2O_3	132	30.3	1.06	7.09	95.0	0.102	2
20%Ni/CeO_2-Al_2O_3	128	29.5	1.16	7.71	87.4	0.442	31
40%Ni/CeO_2-Al_2O_3	78	17.9	0.54	3.61	186	0.414	98
40%Ni/Al_2O_3	133	30.5	0.69	4.63	146	0.326	20.5
40%Ni/CeO_2	34	7.8	0.63	4.18	146	0.479	85
60%Ni/CeO_2-Al_2O_3	58	13.2	0.28	1.90	356	0.531	77
2%Pd-40%Ni/CeO_2-Al_2O_3	42	9.6	-	-	-	-	99.9

Activation of catalysts: reduction before activity tests in the 5 % H_2-95 % Ar mixture at 300 °C, 2 h. Reaction conditions: T = 250 °C, mcat. = 0.2 g, $CH_3OH/H_2O/O_2$ = 1, feed flow rate = 40 mL/min

^{a}Methanol conversion at T = 250 °C

Chemisorption measurements performed for nickel catalysts showed that the highest nickel dispersion degree had 20%Ni/CeO_2-Al_2O_3 catalyst. The lowest dispersion degree showed 60%Ni/CeO_2-Al_2O_3 catalyst. It should be also mentioned that the 20%Ni/CeO_2-Al_2O_3 catalyst had the highest metallic nickel surface area and exhibited the highest amount of hydrogen adsorbed on the metallic nickel atoms (see Table 2). The highest dispersion degree of Ni showed 40%Ni/Al_2O_3 supported catalyst compared to the rest investigated systems. It is worth mentioning, that this system exhibited also the lowest methanol conversion at 250 °C among of all nickel catalysts with the same content of Ni. These results suggest that the size of the metallic particles is not a major factor influencing the reactivity properties of the nickel catalyst in OSRM reaction. The evidence of this is the highest methanol conversion of 40%Ni/CeO_2-Al_2O_3 catalyst in oxy-steam reforming of methanol at 250 °C (see Table 2).

2.3. Reduction behaviour of monometallic Ni and bimetallic Pd-Ni supported catalysts

The temperature programmed reduction studies were performed in order to determine the reducibility of supports (CeO_2 and CeO_2 – Al_2O_3) and Ni supported catalysts. All TPR-H_2 curves recorded for the investigated samples were given in Figure 2A and 2B, respectively. In the first step,

Peer-reviewed version available at *Catalysts* **2018**, *8*, 380; doi:10.3390/catal8090380

the reduction behaviour of CeO_2 was investigated. The result of the TPR-H_2 study is shown in Figure 2A. TPR-H_2 curve recorded for CeO_2 oxide system showed two reduction stages. The first hydrogen consumption peak visible in the temperature range 355-580 °C is connected with the reduction of CeO_2 surface species to non-stoichiometric oxides CeO_{2-x}. The second high-temperature peak located above 670°C is assigned to the bulk CeO_2 reduction **[44]**. Analogous measurement was carried out also for binary oxide. The TPR-H_2 curve showed the same reduction sages which were observed for monoxide CeO_2. Reducibility of nickel catalysts supported on monoxide such as Al_2O_3 and CeO_2 or binary oxide system has also been studied. The TPR-H_2 profile of Ni/Al_2O_3 catalyst showed four hydrogen consumption peaks located at about 270, 420, 545 and 750°C, respectively. The observed reduction effects can be associated with the reduction of various nickel (II) oxide species (see Figure 2A). The first peak located at about 270 °C is connected with the reduction of free NiO species[45]. The second peak with a maximum reduction rate at 420 °C is assigned to the reduction of NiO interacted with support **[46]**. The third hydrogen consumption peak centered at 545°C is assigned to the reduction of Ni-O-Al linkage species **[47-49]**. The last reduction stage above 650°C is assigned to the reduction of spinel phase $NiAl_2O_4$. The reduction behaviour of Ni/Al_2O_3 was also studied previously in work [33], and the authors observed also four reduction stages on the TPR profile recorded for Ni/Al_2O_3 catalyst. The first peak on the TPR-H_2 profile located at about 470 °C they assigned to the reduction of highly dispersed NiO species. The next hydrogen consumption peak positioned at 500 °C authors attributed to the reduction of free and aggregated NiO species. The reduction peak situated at around 550 - 600 °C they attributed to the reduction of both NiO interacted with support and $NiAl_xO_y$ species reduction. The last high temperature reduction effect situated above 800°C was assigned to the $NiAl_2O_4$ species reduction **[48]**.

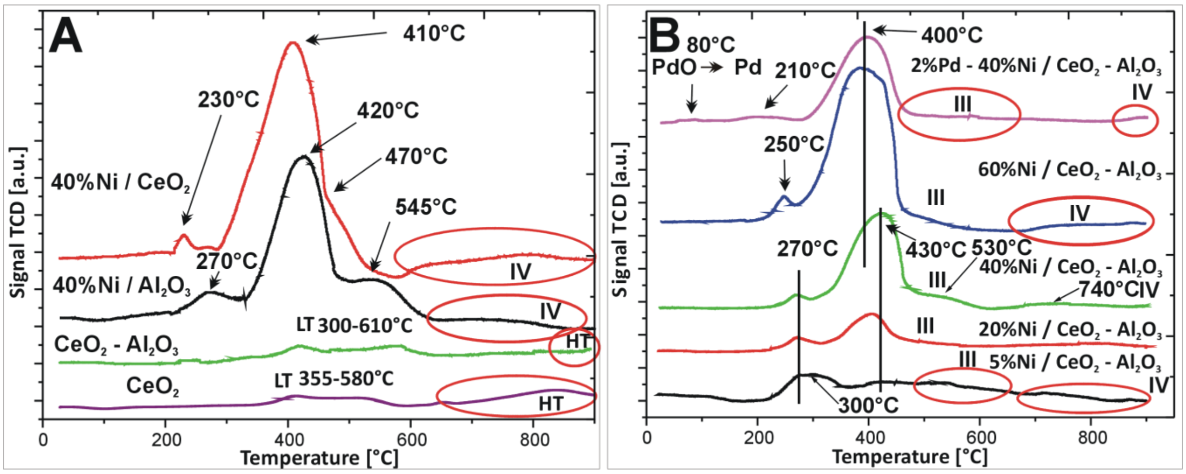

Figure 2. TPR profile of A) supports CeO_2, CeO_2-Al_2O_3 and monometallic catalysts supported on CeO_2 or Al_2O_3 and B) monometallic nickel catalysts supported on binary oxide and bimetallic systems after calcination in air atmosphere for 4h at 400 °C.

The reduction behaviour of Ni/CeO_2 catalyst was also studied in detail. The TPR profile recorded for the system showed its four steps reduction (see Figure 2A). The first two effects are assigned to the reduction of free unbounded and strongly interacted NiO with support. The same reduction stages which were observed for nickel catalyst supported on Ni/Al_2O_3 catalyst [47]. The third stage is assigned to the reduction of surface oxygen species of CeO_2. The last high temperature peak is attributed to the reduction of CeO_2 in bulk [44]. Ahmed et al. [33] also studied the reduction behaviour of Ni catalyst supported on pure CeO_2 and they have reported about two-step reduction process of the nickel supported catalyst. The reduction stages located in the temperature range 300-550 °C are assigned to the Ce^{4+} and also with the reduction of NiO interacted with support. While, any high temperature effect connected with the reduction of bulk Ce^{4+} to Ce^{3+} was not observed on the TPR-H_2 profile.

Peer-reviewed version available at Catalysts 2018, 8, 380; doi:10.3390/catal8090380

In the next step, the interaction between active phase component and support (CeO_2-Al_2O_3) was investigated for the monometallic nickel and bimetallic Pd-Ni catalysts (see Figure 2B). TPR profiles of nickel catalysts supported on CeO_2-Al_2O_3 oxide showed four reduction stages on the reduction profiles independently on the nickel content. TPR profile recorded for 5%Ni/CeO_2-Al_2O_3 catalyst showed the first two reduction stages positioned at 300 and 430°C which are assigned to the reduction of unbounded and strongly interacted with support NiO species. The third reduction peak located in the temperature range 500-650°C is attributed to the reduction of surface oxygen species of CeO_2 and Ni-O-Al linkage reduction. The last reduction stage is attributed to the reduction of CeO_2 in bulk as well as to the reduction of spinel $NiAl_2O_4$ structure. TPR curve of 20%Ni/CeO_2-Al_2O_3 system showed also four stages, which are connected with the same oxides species reduction. The first two reduction peaks were visible at 270 and 430°C, respectively. While, the third effect is located in the temperature range 480-600°C and the last one is situated above 650 and is finished up to 900°C. Further increase of the Ni content in the catalytic systems did not change the reduction behaviour of the investigated nickel catalysts. TPR profile of 40%Ni/CeO_2-Al_2O_3 was the same shape as previously described Ni catalyst. On the other hand, the TPR curve of 60%Ni/CeO_2-Al_2O_3 catalyst exhibited the same reduction stages as for previously presented catalysts the only difference was the location of each effects and their intensity. In the case of 60%Ni/CeO_2-Al_2O_3 catalyst first two effects were visible at 250 and 400°C and their intensity were significantly higher compared to previously described systems. While, the third effect was located in the temperature range 450-600°C. The last high temperature effect (IV) connected with the reduction of CeO_2 in bulk as well as to the reduction of spinel $NiAl_2O_4$ structure was observed above 680°C. The reduction process of monometallic Ni catalysts supported on CeO_2-Al_2O_3 system containing various Ce/Al ratio content was investigated previously [33]. The authors reported that their reducible behaviour strongly depend on the catalyst composition. They have found four stages on the TPR profile recorded for Ni catalysts. The first two situated at about 400 and 410 °C were assigned to the reduction of the bulk NiO species scarcely interacting with γ-Al_2O_3 and free NiO species, respectively. The high temperature hydrogen consumption peaks located at 729 and 827 °C were assigned with NiO_x which strongly interacted with γ-Al_2O_3 and highly dispersed $NiAl_2O_4$. The reducibility of Ni catalysts supported on CeO_2, Al_2O_3 and CeO_2-Al_2O_3 supports were studied earlier also in work[50]. The authors have found several reduction peaks in the investigated temperature range of 350 - 900 °C. The remaining reduction peaks were assigned to three types of NiO species (α, β and γ) depending on the reduction temperatures, respectively. The α-type is assigned to the reduction of free NiO species (350 - 450 °C). The β-type is attributed to the reduction of NiO species interacted with Al_2O_3 support and the reduction peak is located in the temperature range 450 - 750 °C. The peak at the high temperature (750 - 850 °C) is attributed to the less reducible $NiAl_2O_4$ spinel phase. The reduction profile of Ni/Al_2O_3 catalyst showed only the reduction peaks in the temperature region of 500 - 850 °C. The occurrence of the TPR-H_2 peaks assigned to β-type and γ-type, confirmed the hard reducible types of NiO species interacting with Al_2O_3. In the case of nickel catalysts supported on binary oxide (CeO_2-Al_2O_3) the observed reduction peaks were shifted towards lower temperature. The shift of the effects means that addition of CeO_2 into Al_2O_3 weakness the interaction between the NiO and Al_2O_3. TPR-H_2 profile of Ni/CeO_2 showed the main reduction peak at 350 - 450 °C attributed to α-type of NiO species reduction. The last catalytic system which was studied by temperature-programmed-reduction technique was bimetallic Pd-Ni/CeO_2-Al_2O_3 supported catalyst. The TPR-H_2 profile of bimetallic catalyst showed five effects on reduction profile. The first reduction step positioned at 80°C is assigned to the reduction of PdO to metallic palladium. Second and third hydrogen consumption peak located at 210 and 400°C are assigned to the reduction of unbounded and strongly interacted with support NiO species. This means that addition of palladium into nickel supported catalyst facilitates the reduction of NiO species what is confirmed by the shift of the second and third observed reduction profiles towards lower temperature range compared to the same reduction effects observed in the case of monometallic 40%Ni/CeO_2-Al_2O_3 catalyst. The fourth and fifth hydrogen consumption peaks are positioned at the same temperature as for 40%Ni/CeO_2-Al_2O_3 catalyst. The shift of the visible second and third effect recorded in the case of bimetallic supported catalysts

Peer-reviewed version available at *Catalysts* **2018**, *8*, 380; doi:10.3390/catal8090380

compared to monometallic catalyst towards low temperature range is due to spillover phenomena occurring between metallic palladium and nickel oxide. Hydrogen dissociates on palladium and then atomic hydrogen spills over from metallic palladium to nickel oxide causing its reduction.

2.4. XRD structural analysis

The analysis of the diffraction curves recorded for monometallic nickel supported catalysts calcined in air for 4h at 400 °C showed the presence of only NiO and CeO_2 phases independently of the nickel content. This is supported in the published works **[51, 52]**. Ahmed at al. [33] studied the phase composition of the as prepared CeO_2-Al_2O_3 binary oxide and mono- oxides such as: CeO_2 and Al_2O_3 supports calcined in air at 550 °C. The XRD analysis of alumina showed only broad and weak peaks between 30 and 40° which were assigned to θ-Al_2O_3 phase and additional weak peaks attributed to γ-Al_2O_3 phase. Broadened diffraction peaks confirmed the amorphous state of the alumina oxide. The analogical analysis carried out for pure CeO_2 confirmed the occurrence of peaks assigned to crystalline CeO_2 cubic fluorite structure at 2θ of 28.5°, 33.2°, 47.8° and 56.7°.

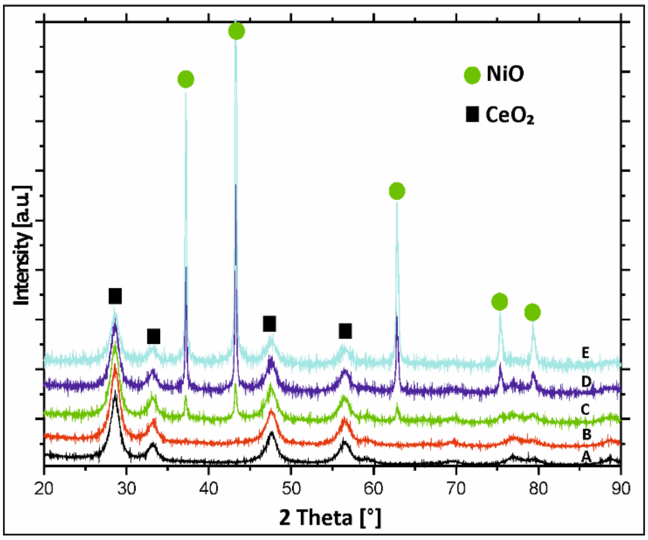

Figure 3. X-ray powder patterns of calcined A) binary oxide and monometallic B) 5%Ni/CeO_2-Al_2O_3, C) 20%Ni/CeO_2-Al_2O_3, D) 40%Ni/CeO_2-Al_2O_3 and E) 60%Ni/CeO_2-Al_2O_3 catalysts in an air atmosphere for 4h at a temperature of 400 °C.

Analogous phase composition studies were performed for binary oxide CeO_2-Al_2O_3 systems containing various content of CeO_2. The analysis showed that in parallel to the CeO_2 content increase in the binary oxide system, the main peak of CeO_2 fluorite structure became sharper and stronger, which indicates that this oxide better crystallized on the surface of aluminum oxide **[53]**. No other phases were observed on the diffraction patterns recorded for other binary oxide systems.

Peer-reviewed version available at Catalysts 2018, 8, 380; doi:10.3390/catal8090380

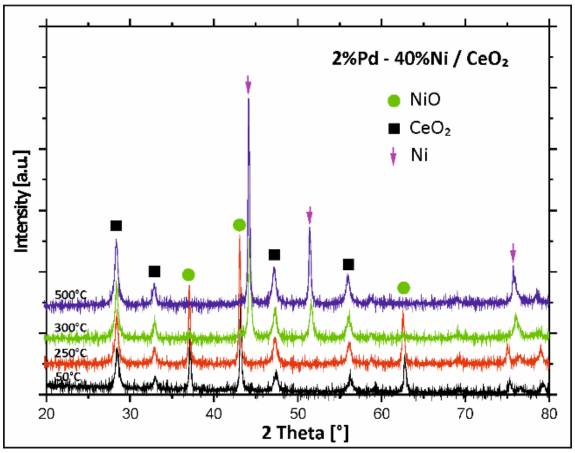

Figure 4. X-ray powder patterns recorded during reduction of calcined bimetallic Pd-Ni/CeO_2 catalyst in a mixture of 5%H_2-95%Ar in the temperature range 50-500 °C.

To study the changes of the phase composition during the activation process performed before the catalytic tests and to explain the reduction behaviour of the mono and bimetallic catalysts supported on binary oxide,,in situ" XRD measurements in a mixture of 5%H_2-95%Ar were carried out in the temperature range 50-500 °C for bimetallic catalysts supported on mono Al_2O_3, CeO_2 and binary oxide CeO_2-Al_2O_3. Bimetallic Pd-Ni/CeO_2 catalyst was first tested. Results are given in Figure 4. The analysis of the diffraction curves recorded for bimetallic Pd-Ni catalyst supported on CeO_2 showed that from 50 °C to 250 °C the diffraction curves showed only NiO and CeO_2 phases on the diffractograms. The increase of the reduction temperature above 250 °C results in disappearance of the NiO phase. The XRD pattern recorded at 300°C for Pd-Ni/CeO_2 catalyst showed the diffraction peaks of metallic nickel and CeO_2 phases. It should be also noted that at 250 °C the diffraction peaks assigned to the NiO phase as a minor phase were visible. Further increasing of the reduction temperature above 300 °C caused the occurrence of CeO_2 and metallic nickel phases on the diffraction curves. In the next step of the XRD „in situ" measurements Pd-Ni/Al_2O_3 bimetallic supported catalysts were studied and the diffraction curves obtained in the investigated temperature range are presented in Figure 5.

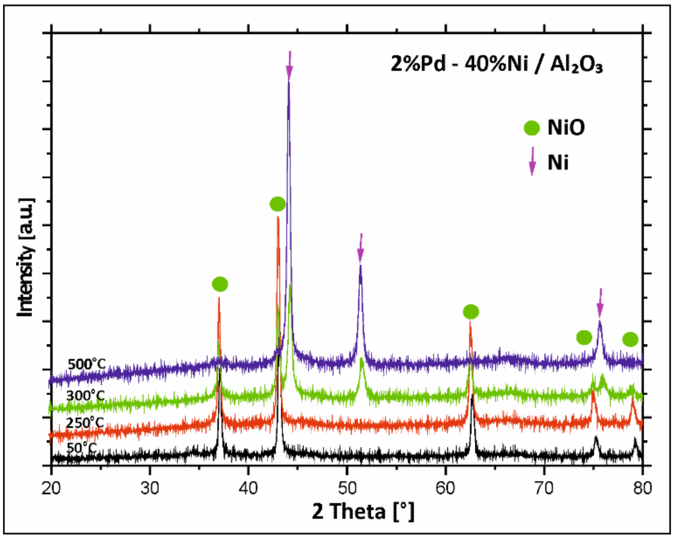

Figure 5. X-ray powder patterns recorded during reduction of calcined bimetallic Pd-Ni/Al_2O_3 catalyst in a mixture of 5%H_2-95%Ar in the temperature range 50-500 °C.

Analogous measurements were performed in the same temperature range for Pd-Ni/Al_2O_3 catalyst. At starting temperature (50 °C) the diffraction pattern showed the existence the NiO phase.

Peer-reviewed version available at Catalysts 2018, 8, 380; doi:10.3390/catal8090380

At 300 °C, additional metallic nickel phase was detected on the diffraction curve. Increasing the reduction temperature above 300 °C showed the disappearance of the diffraction peaks assigned to NiO phase. At final reduction temperature of 500 °C only metallic nickel phase was detected. The lack of the γ-Al_2O_3 is explained by the high amorphousness of this phase.

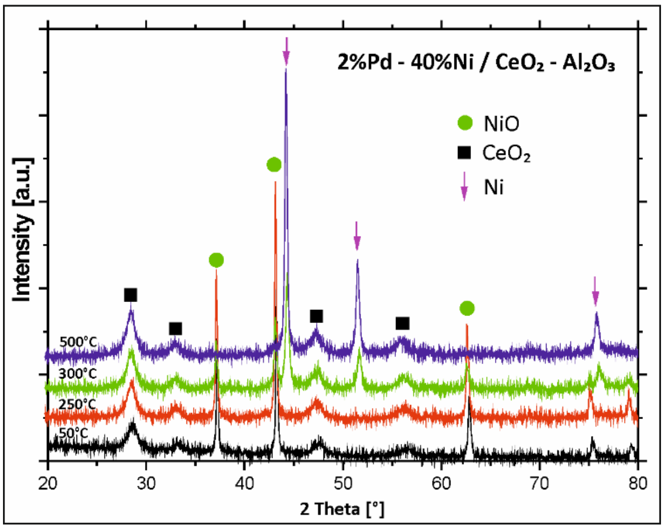

Figure 6. X-ray powder patterns recorded during reduction of calcined bimetallic Pd-Ni/CeO_2-Al_2O_3 catalyst in a mixture of 5%H_2-95%Ar in the temperature range 50-500 °C.

Figure 6 presents the phase composition studies performed for Pd-Ni/CeO_2-Al_2O_3 catalyst. The analysis of the X-ray diffraction measurements performed for bimetallic catalysts supported on binary oxide CeO_2-Al_2O_3 showed the existence of NiO and CeO_2 phases at temperature below 250 °C. The increase of the activation process temperature to 300 °C results in appearance of the additional metallic nickel phase. Further temperature increase, above 300 °C cause disappearance of the diffraction peaks assigned to NiO phase and the presence of reflexes originating from the metallic Ni and CeO_2 phases. Summarizing, the „in situ" X-ray diffraction measurements performed for all bimetallic catalysts in a temperature range 50-500 °C confirmed the proposed reduction mechanism of NiO species describing above for mono and bimetallic Pd-Ni catalyst supported on CeO_2-Al_2O_3 binary oxide. The results confirmed two steps of nickel (II) oxide reduction through a reduction of unbounded and interacting with the carrier NiO species. In addition, it should be also emphasized, that metallic Pd phase was not visible on the diffraction curves recorded for all bimetallic supported catalysts. The lack of the diffraction peaks assigned to metallic Pd phase on diffraction curves means that Pd particles has too small size to detect by XRD technique.

2.5. Temperature programmed desorption of ammonia TPD-NH_3

The total acidity and the distribution of acid centres calculated based on the area under the peak situated at an appropriate desorption temperature of the prepared catalysts were studied using temperature-programmed desorption of ammonia. TPD-NH_3 experiments were performed in order to elucidate the influence of Ni and Pd on the acidity of the prepared systems and to determine the role of their acidity on the catalytic activity in the process of oxy-steam reforming of methanol. It is well known that the acidity centers play crucial role during reforming of methanol.

Preprints (www.preprints.org) | NOT PEER-REVIEWED | Posted: 2 August 2018 doi:10.20944/preprints201808.0050.v1

Peer-reviewed version available at *Catalysts* **2018**, *8*, 380; doi:10.3390/catal8090380

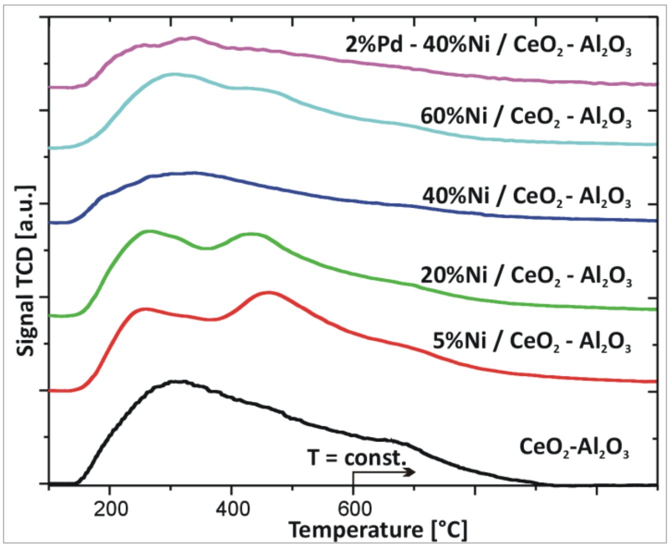

Figure 7. TPD-NH_3 profile of the binary oxide and monometallic catalysts after calcination in air for 4 h at 400°C.

The acidity centers are involved in the stabilization of intermediates formed during reforming of methanol process. The rate and amount of the formed intermediates such as: methoxy, formate and carbonate species significantly affect the catalytic activity of the studied systems in oxy-steam reforming of methanol reaction. The results of the surface acidity obtained for all investigated catalytic systems are given in Table 3 and Figure 7. TPD-NH_3 measurements performed over support material, monometallic and bimetallic supported catalysts indicated that the total surface acidity of all studied systems was in the range of 0.26 - 0.63 mmol $NH_3 \cdot g^{-1}_{cat}$. Binary oxide itself showed the total acidity of 0.59 mmol$\cdot g^{-1}_{cat.}$. The introduction of a small amount of nickel into the support surface results in a slight increase of the total acidity of the formed catalyst. Further increasing of the metal content causes its surface acidity decrease. The lowest total acidity among all the nickel catalysts supported on CeO_2-Al_2O_3 showed 40% Ni/CeO_2-Al_2O_3 catalyst. In contrast, comparison of the acidity of nickel catalysts supported on mono- Al_2O_3 or CeO_2 and binary oxide CeO_2-Al_2O_3 showed that the highest acidity exhibited Ni/Al_2O_3 catalyst. While, the lowest value of total ammonia desorbed from the catalyst surface showed Ni/CeO_2 system, the intermediate value of total acidity had 40%Ni/CeO_2-Al_2O_3 catalyst. Total acidity of the nickel catalysts supported on alumina and ceria-alumina oxides were also measured by NH_3-TPD by Reyes et al. **[52]**. The results of the acidity showed that high addition of Ce (>10 wt%) caused the decrease of the total acidity. The authors reported that CeO_2 introduction into the γ-Al_2O_3 mono- oxide reduces the amount and strength of the acidic sites. The acidity of the nickel supported catalysts was also studied by Jiao et. al. **[54]**. All of the supported nickel catalysts showed as in our case, three or four strong desorption peaks in the temperature range 100 - 500 C. It is also worth mentioning that the largest desorption peaks contain the weak and medium acid centres. The authors also obtained similar results. They have found that the amount of acid centres decrease parallel with the addition of metal Ni. The catalytic activity is dependent on the acidity of the system and the strength of the acidic centers present in the tested catalyst. The process of the oxy-steam reforming of methanol was carried out up to 250°C what means that medium-strength and strong acid sites do not take part in the reaction due to their incapability to adsorb of methanol at low temperature range. Based on this assumption, only weak strength centres can take part in the stabilization process of the intermediates over nickel catalysts supported on CeO_2, Al_2O_3 and CeO_2-Al_2O_3 systems created during the reaction. The acidity results obtained for investigated catalysts indicate that catalytic systems exhibited acidity at a temperature of 100-300 °C in the range from 0.07 to 0.13 mmol of desorbed ammonia per gram of the catalyst. It should be also noted that poorly active systems 5%Ni/CeO_2-Al_2O_3 and 20%Ni/Al_2O_3 showed the highest values of acidity equal 0.12 and 0.13 mmol/g cat., respectively. This means that some limited acidity is required to achieve highly active systems in the studied process, but too high value of acid centers have negative impact on the catalytic activity. Too many acid centers lead to methanol decomposition to methoxy and methyl groups, eventually leading to dimethyl ether formation (see Table 1).

Table 3. The amount of NH_3 adsorbed on supports, monometallic nickel and bimetallic Pd-Ni/CeO_2-Al_2O_3 catalysts calcined in air atmosphere at 400 °C from the TPD-NH_3 data.

Catalysts/Supports	**weak centers [mmol/g] 100-300 °C**	**medium centers [mmol/g] 300-450 °C**	**strong centers [mmol/g] 450-600 °C**	**Total acidity [mmol/g] 100-600 °C**
CeO_2-Al_2O_3	0.13	0.19	0.27	0.59
5%Ni/CeO_2-Al_2O_3	0.12	0.17	0.34	0.63
20%Ni/CeO_2-Al_2O_3	0.12	0.16	0.28	0.56
40%Ni/CeO_2-Al_2O_3	0.07	0.10	0.13	0.30
60%Ni/CeO_2-Al_2O_3	0.09	0.14	0.18	0.41
40%Ni/CeO_2	0.07	0.07	0.12	0.26
40%Ni/Al_2O_3	0.13	0.15	0.24	0.52
2%Pd-40%Ni/CeO_2-Al_2O_3	0.06	0.09	0.13	0.28

2.6. Morphology studies of mono and bimetallic supported catalysts using SEM-EDS

The morphology and the elemental composition of the bimetallic 2%Pd-40%Ni catalysts supported on mono- Al_2O_3, CeO_2 and binary oxide CeO_2-Al_2O_3 were extensively studied by a scanning electron microscope, equipped with an energy dispersive spectrometer EDS. The results of the SEM-EDS measurements performed for bimetallic catalyst supported on alumina calcined at 400 °C are given in Figure 8.

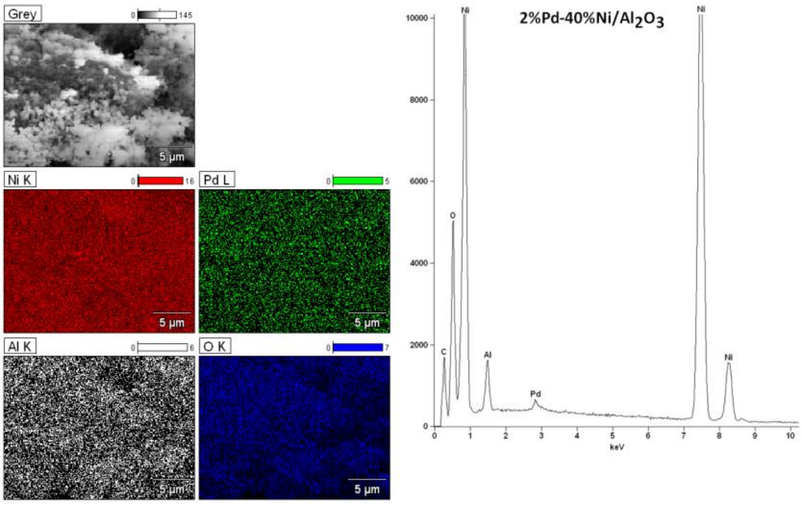

Figure 8. SEM images and EDS spectra for the bimetallic 2%Pd-40%Ni/Al_2O_3 catalysts calcined at 400 °C in air atmosphere for 4h.

Peer-reviewed version available at Catalysts 2018, 8, 380; doi:10.3390/catal8090380

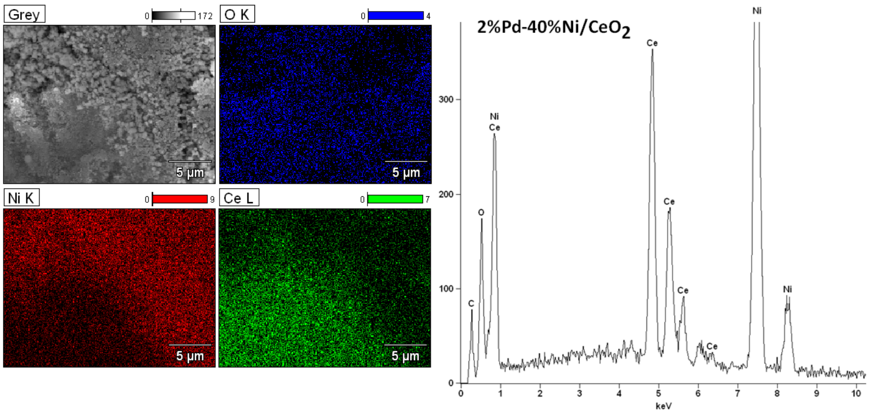

Figure 9. SEM images and EDS spectra for the bimetallic 2%Pd-40%Ni/Ce_2O_3 catalysts calcined at 400 °C in air atmosphere for 4h.

The magnification during the analysis of bimetallic catalytic system was 5000. The surface analysis performed for bimetallic catalyst showed the occurrence of nickel, aluminium, oxygen and palladium on the catalytic surface. Figure 9 presents the analogous measurements carried out for bimetallic catalyst supported on CeO_2 system after calcination at 400 °C in air atmosphere. The EDS spectrum collected form the surface confirmed the occurrence of nickel, ceria and oxygen. The lack of the palladium would suggest the covering of this element by other catalyst components on the investigated catalyst surface. In order to investigate the elemental composition of the catalyst the same measurements were performed for bimetallic catalyst supported on binary oxide. The surface analysis of bimetallic Pd-Ni/CeO_2-Al_2O_3 catalyst calcined at 400 °C in an air showed similar results. The only difference was the occurrence of aluminium on the catalyst surface. Additionally, the regions on which cerium and aluminium elements are present can be easily distinguished. This result can be explained by a specific interaction which occurs between CeO_2 and Al_2O_3 oxides and which could be confirmed by the reduction results obtained for the systems supported on CeO_2-Al_2O_3 binary oxide.

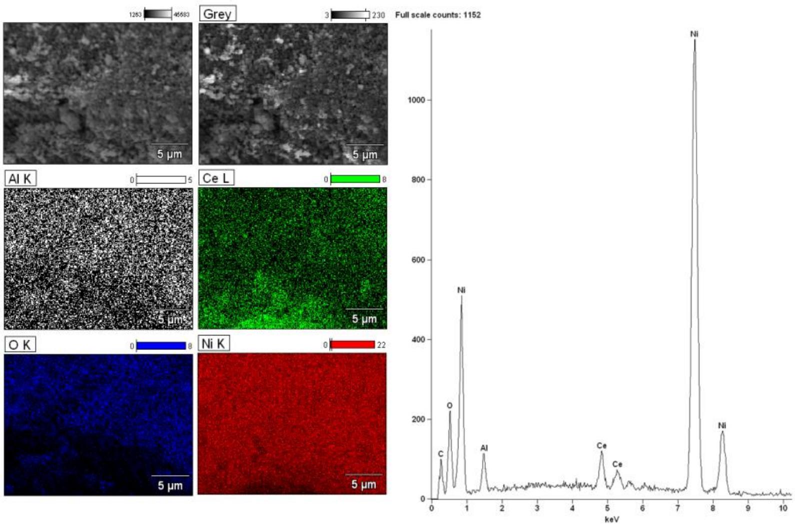

Figure 10. SEM images and EDS spectra for the bimetallic 2%Pd-40%Ni/CeO_2-Al_2O_3 catalysts calcined at 400 °C in air atmosphere for 4h.

2.7. Interaction between the active phase component and support

X-ray photoelectron spectroscopy (XPS) was used to study the electronic structure and the chemical surface composition of the catalytic material. This technique is a very powerful method to

Peer-reviewed version available at Catalysts 2018, 8, 380; doi:10.3390/catal8090380

study the changes in the electronic structure of the active phase component supported on various support surfaces. In this work, the electronic structural changes of Ni after promotion of monometallic nickel catalyst by palladium were investigated.

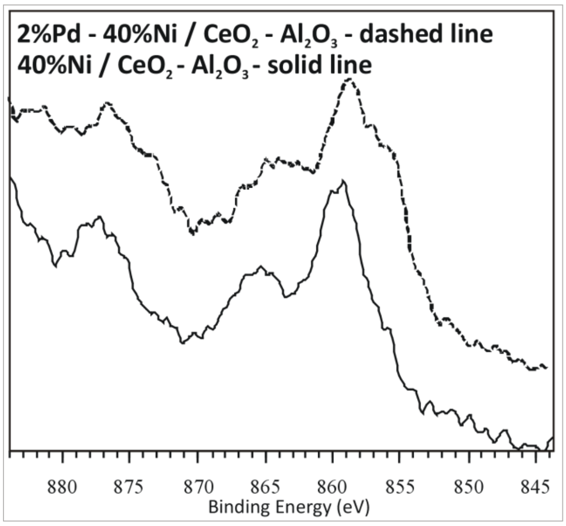

Figure 11. Ni 2p XPS spectra of A) 40%Ni/CeO_2-Al_2O_3 and 2%Pd-40%Ni/CeO_2-Al_2O_3 reduced in a mixture of 5%H_2-95%Ar at 500 °C.

In order to elucidate the interaction between the active phase component and/or support the X-ray photoelectron spectroscopy analysis was carried out for monometallic Ni and bimetallic 2%Pd-40%Ni/CeO_2-Al_2O_3 after reduction in a mixture of 5%H_2-95%Ar at 500 °C. The XPS high resolution spectra of the binding energies between 844 and 884 eV show several characteristic peaks. The peak in the region of 844 - 884 eV includes Ni^{2+} species (857 eV), metallic nickel (853 eV). The typical position of the XPS bands which confirms the occurrence of Ni^{2+} and Ni^0 in the sample is 856 and 852.8 eV, respectively. The shift of the observed band assigned to the Ni^{2+} towards higher binding energy indicates that most of the nickel is in its oxidized or charged states. For our investigated catalysts the observed shifts of the specific bands is connected with the interaction which take place between NiO and Al_2O_3 or CeO_2 monoxides. This result confirmed the observed reduction profiles on the TPR-H_2 curves recorded for monometallic and bimetallic catalysts supported on CeO_2-Al_2O_3 binary oxide system. Luisetto et al. [55] studied the Ni catalysts supported on CeO_2-Al_2O_3 system by XPS technique. They reported about complicated Ni2p spectra due to the presence of high BE satellites. The calcined sample showed the main peak situated at a BE value of 854 eV which was attributed to the Ni^{2+} species. The shift of this peak related to the typical signal positioned at 856 was explained by the high interaction with the support. The XPS analysis performed by the authors for reduced catalyst showed the characteristic band assigned to the metallic nickel at lower BE values located at about Ni $2p_{3/2}$ = 853.0 - 853.5 eV. The observed shift can be associated with the partial oxidation of the sample before the real measurement.

3. Experimental

3.1. Catalytic material preparation

3.1.1 Support material

Monoxide such as: Al_2O_3 or CeO_2 were prepared by precipitation method using ammonia as a precipitation agent. The resulting solid obtained after precipitation process was aged for 12 hours. Then final precipitates were washed two times in deionized water and dried at 120 °C for 15 h in an air atmosphere. Then in the next step, the obtained supports were calcined in air atmosphere for 4 h at 400 °C.

Peer-reviewed version available at Catalysts 2018, 8, 380; doi:10.3390/catal8090380

The CeO_2-Al_2O_3 support with a Ce : Al molar ratio of 1 : 2, was prepared by precipitated method. Aluminum and cerium nitrates were used during the co-precipitation step. A concentrated ammonia solution was used as a precipitation agent and was added dropwise until the pH reached values between 10 and 11. Then, the resulting mixtures were stirred for another 30 minutes. The resulting precipitate was then aged for 12 hours and after that it was washed two times in deionized water, dried at 120 °C for 15 h, and calcined in air for 4 h at 400 °C.

3.1.2 Preparation of supported monometallic and bimetallic catalysts

Nickel supported catalysts were prepared by conventional wet aqueous impregnation method. NiO phase was introduced on the support (CeO_2-Al_2O_3, CeO_2, Al_2O_3) surface by wet impregnation method from the nickel nitrate (V) aqueous solutions. Then the obtained systems were dried for 2h at 120 °C in an air atmosphere and finally calcined for 4 h in air atmosphere at 400 °C. Palladium phase was introduced on Ni/support catalysts surface by consequence impregnation method using $Pd(NO_3)_2$ solution. Then bimetallic systems were dried for 2h in air atmosphere at 120 °C, and then calcined at 400 °C for 4h at the same atmosphere. Nickel and palladium content in the catalytic material were 5, 20, 40 and 60 wt. % of Ni and 2 wt. % of Pd, respectively.

3.2. Catalytic material characterization

The BET surface area and porosity of catalytic materials were determined in a sorptometer Sorptomatic 1900 apparatus. Reducibility of the prepared catalysts were studying by temperature-programmed-reduction measurements were carried out in an automatic AMI-1 instrument in the temperature range of 25 - 900 °C with a heating rate of 10 °C min^{-1}. The mass of the sample in each test was about ~ 0.1 g. The investigated materials were reduced in a mixture of 5% H_2 - 95% Ar with a volumetric flow rate of 40 cm^3/min. Hydrogen consumption was measured using a thermal conductivity detector. Phase composition studies of the catalysts were studied using a PANalyticalX'Pert Pro MPD diffractometer in Bragg-Brentano reflecting geometry. CuKα radiation from a sealed tube was applied during all measurements. Obtained data were collected in the 2θ angle 5 - 90°. All calculations during analysis have been carried out using X'PertHighScore Plus computer software. In addition, the phase composition studies of the selected Pd-Ni bimetallic catalysts during the reduction in a mixture of a 5% H_2-95% Ar in the temperature range 50-500 °C were carried out in a PANalyticalX'Pert Pro diffractometer equipped with an Anton Paar XRK900 reactor chamber. During each measurement a PANalyticalX'Celerator detector based on Real Time Multiple Strip technology was used. The acidity of the prepared catalysts was studied by TPD-NH_3 technique. Prior to each measurement the sample surface was previously purified in flowing He at 600 °C for 60 min. Then the NH_3 was adsorbed on the catalyst surface at 50 °C for 30 min. Afterward, the physically adsorbed NH_3 was removed from the surface in a helium stream at 100 °C. Then in the next step, the chemically adsorbed NH_3 on the catalyst surface was determined using temperature programmed desorption process in the temperature range 100-600 °C with a heating rate of 25 °C min-1. A thermal-conductivity detector was used to monitor the concentration of the chemically desorbed ammonia from the surface of the investigated sample. Hydrogen chemisorption measurements were performed in a Micromeritics ASAP 2020 apparatus. Before the appropriate H_2 chemisorption process, each catalytic material was reduced in situ at 500 °C in a mixture of 5 % H_2-95 % Ar for 2 h. Then the samples were cooled to 35 °C under inert gas (He). In the following step the amount of the chemisorbed hydrogen was determined using the adsorption-backsorption isotherm method. The Scanning Electron Microscope (S-4700 HITACHI, Japan) equipped with EDX detector (ThermoNoran, USA) was used to measure the surface morphology for the selected micro-area of the bimetallic catalysts. The surface analysis was carried out at several magnifications. Qualitative analysis of the micro-area of the sample surface layer was carried out based on the X-ray spectra. The distributions of the each element on the studied micro-area were analysed. The accelerating voltage applied during the investigations was 25 kV. A Specs SAGE XPS spectrometer was used to study the

Peer-reviewed version available at *Catalysts* **2018**, *8*, 380; doi:10.3390/catal8090380

electronic structure of the active phase component. Spectrometer operated at 10 kV and 20 mA using Mg Kα radiation source (h=1253.6 eV) in each measurement. The high-resolution spectra were analysed using CasaXPS software.

3.3. Catalytic activity evaluation

The oxy-steam reforming of methanol process was carried out using a flow quartz micro-reactor under atmospheric pressure at a temperature of 200 and 250 °C, respectively. The composition of the reaction mixture used in each catalytic test was as follows $H_2O/CH_3OH/O_2$= 1/1/0.4 (molar ratio) and the GHSV was 26700 h^{-1} (calculated at ambient temperature and under atmospheric pressure). The total flow-rate was kept at 31.5 ml/min and the Ar was used as the balance gas (the methanol content in the reaction mixture was 6%). The reaction mixture was prepared using two saturators. One was used to saturate argon in methanol vapour and the second one was used to saturate the mixture of 5% O_2-95% Ar in steam. The flow of the mixed gases was controlled by flow meters. Before introduction into the micro-reactor both gases were mixed. The reaction mixture leaving the micro-reactor was directed to the first GC equipped with FID detector where the methanol conversion and the concentration of others organics compounds were evaluated. Then the mixture was passed through the steam trap and was directed to the second and third GC where hydrogen and other products (CO, CO_2) were monitored, respectively [1]. The activity measurements were taken after two hours of stabilization at each temperature. The mass of the catalyst used in each test was 0.2 g [1]. The analysis of the reaction organic products (methanol, methane, methyl formate, dimethylether (DME), and formaldehyde) was carried out by an on-line gas chromatograph equipped with FID detector and 10 %Carbowax 1500 on Graphpac column. While, CO and CO_2 concentrations were followed by GC chromatograph equipped with TCD detector (150°C, 60 mA), and Carbosphere 60/80 (50°C) column. The hydrogen concentration was measured by a GC chromatograph equipped with TCD detector (120°C, 60 mA) and molecular sieve 5a (120°C) column. In each experiment material balances on carbon were calculated to verify the obtained results. The selectivity results for all catalysts towards the formation of hydrogen, carbon monoxide, carbon dioxide and DME in OSRM was calculated using Eq. 1, 2, 3, 4 and the conversion of methanol using Eq. (5):

$$S_{H_2}(\%) = \frac{(nH_{2-out})}{\sum products\ of\ the\ reaction}*100 \qquad (1).$$

$$S_{CO}(\%) = \frac{(nCO_{out})}{\sum products\ of\ the\ reaction}*100 \qquad (2).$$

$$S_{CO_2}(\%) = \frac{(nCO_{2-out})}{\sum products\ of\ the\ reaction} * 100 \qquad (3).$$

$$S_{DME}(\%) = \frac{(nDME_{out})}{\sum products\ of\ the\ reaction}*100 \qquad (4).$$

Where, n CH_3OH and n H_2 is the molar flow rate of CH_3OH and H_2, respectively.

$$Conv._{CH_3OH}(\%) = \frac{n_1^{in}CH_3OH - n_2^{out}CH_3OH}{n_1^{in}CH_3OH}*100 \qquad (5).$$

Where,

$nH_{2\text{-}out}$- molar flow rate of H_2 feed out,

$nCO_{2\text{-}out}$- molar flow rate of CO_2 feed out,

nCO_{out}- molar flow rate of CO feed out,

Peer-reviewed version available at Catalysts 2018, 8, 380; doi:10.3390/catal8090380

n_1^{in} CH_3OH, n_2^{out} CH_3OH - molar flow rate of CH_3OH feed in and feed out, respectively. Methane, formaldehyde and methyl formate formation were not observed. Only carbon monoxide, carbon dioxide, hydrogen and DME were formed as reaction products during the process.

4. Conclusions

In summary, the monometallic Ni/CeO_2-Al_2O_3 and bimetallic Pd-Ni/CeO_2-Al_2O_3 catalyst were prepared by impregnation and subsequent impregnation method, respectively. The oxy-steam reforming of methanol reaction has been successfully carried out on monometallic Ni and bimetallic Pd-Ni catalysts supported on binary oxide CeO_2-Al_2O_3 system for hydrogen production. The catalytic activity results performed for all catalysts showed that bimetallic 2%Pd-40%Ni/CeO_2-Al_2O_3 catalyst exhibit the highest activity, stability and the highest selectivity towards hydrogen formation in OSRM process. The reactivity results confirmed the promotion effect of palladium on catalyst activity of Ni supported catalyst. It was also proven that palladium facilitates the reduction of NiO species on catalyst surface by spillover effect occurring between Pd and NiO. The facilitated reduction of NiO species and the generation of additional adsorption centers on the catalyst surface after the introduction of palladium may be responsible for increasing of the catalytic activity and selectivity of the bimetallic catalyst towards hydrogen formation. The performed measurements showed that the activity results strongly depend on the content of nickel in the investigated system and their acidity and reducibility. The experimental results confirmed that both metal active centres and acid sites play crucial role during oxy-steam reforming of methanol. In addition, the acid centres located close to high dispersed metal centres may have significant effect on the catalytic activity of the investigated catalyst. The activity measurements showed that the synthesized palladium-nickel system exhibited high stability in OSRM process which confirms their potential use in fuel cell technology.

Acknowledgements

This work was funded by Polish Ministry of Science and Higher Education within the "Iuventus Plus" Programme (2015-2017) (project no. 0305/IP2/2015/73).

I would like to thank Mr A. Kedziora for help in the research (TPR-H_2, TPD-NH_3, activity tests) carried out in the framework of the work.

Conflicts of Interest: The authors declare no conflict of interest.

References

[1] P. Mierczynski, K. Vasilev, A. Mierczynska, W. Maniukiewicz, M.I. Szynkowska, T.P. Maniecki, Bimetallic Au–Cu, Au–Ni catalysts supported on MWCNTs for oxy-steam reforming of methanol, Applied Catalysis B: Environmental, 185 (2016) 281-294.

[2] R.A. Voloshin, M.V. Rodionova, S.K. Zharmukhamedov, T. Nejat Veziroglu, S.I. Allakhverdiev, Review: Biofuel production from plant and algal biomass, International Journal of Hydrogen Energy, 41 (2016) 17257-17273.

[3] J. Bae, S. Lee, S. Kim, J. Oh, S. Choi, M. Bae, I. Kang, S.P. Katikaneni, Liquid fuel processing for hydrogen production: A review, International Journal of Hydrogen Energy, 41 (2016) 19990-20022.

[4] P. Mierczynski, K. Vasilev, A. Mierczynska, R. Ciesielski, W. Maniukiewicz, J. Rogowski, I.M. Szynkowska, A.Y. Trifonov, S.V. Dubkov, D. Gromov, T.P. Maniecki, The effect of gold on modern bimetallic Au-Cu/MWCNT catalysts for oxy-steam reforming of methanol, Catalysis Science & Technology, (2016).

[5] J. Lu, X. Li, S. He, C. Han, G. Wan, Y. Lei, R. Chen, P. Liu, K. Chen, L. Zhang, Y. Luo, Hydrogen production via methanol steam reforming over Ni-based catalysts: Influences of Lanthanum (La) addition and supports, International Journal of Hydrogen Energy.

[6] P. Mierczynski, R. Ciesielski, A. Kedziora, M. Nowosielska, J. Kubicki, W. Maniukiewicz, A. Czylkowska, T. Maniecki, Monometallic copper catalysts supported on multi-walled carbon nanotubes for the oxy-steam reforming of methanol, Reaction Kinetics, Mechanisms and Catalysis, (2015) 1-17.

[7] X. Liu, J. Toyir, P. Ramírez de la Piscina, N. Homs, Hydrogen production from methanol steam reforming over Al2O3- and ZrO2-modified CuOZnOGa2O3 catalysts, International Journal of Hydrogen Energy.

[8] P. Mierczynski, K. Vasilev, A. Mierczynska, W. Maniukiewicz, T.P. Maniecki, Highly selective Pd–Cu/ZnAl2O4 catalyst for hydrogen production, Applied Catalysis A: General, 479 (2014) 26-34.

[9] D. Liu, Y. Men, J. Wang, G. Kolb, X. Liu, Y. Wang, Q. Sun, Highly active and durable Pt/In2O3/Al2O3 catalysts in methanol steam reforming, International Journal of Hydrogen Energy, 41 (2016) 21990-21999.

[10] P. Mierczynski, K. Vasilev, A. Mierczynska, W. Maniukiewicz, T. Maniecki, The Effect of ZnAl2O4 on the Performance of Cu/ZnxAlyOx+1.5y Supported Catalysts in Steam Reforming of Methanol, Topics in Catalysis, 56 (2013) 1015-1025.

[11] Z. Luo, D. Li, H. Tang, M. Pan, R. Ruan, Degradation behavior of membrane-electrode-assembly materials in 10-cell PEMFC stack, International Journal of Hydrogen Energy, 31 (2006) 1831-1837.

[12] H. Xu, X. Hou, Synergistic effect of CeO2 modified Pt/C electrocatalysts on the performance of PEM fuel cells, International Journal of Hydrogen Energy, 32 (2007) 4397-4401.

[13] P. Mierczynski, Comparative Studies of Bimetallic Ru–Cu, Rh–Cu, Ag–Cu, Ir–Cu Catalysts Supported on ZnO–Al2O3, ZrO2–Al2O3 Systems, Catalysis Letters, (2016) 1-13.

[14] P. López, G. Mondragón-Galicia, M.E. Espinosa-Pesqueira, D. Mendoza-Anaya, M.E. Fernández, A. Gómez-Cortés, J. Bonifacio, G. Martínez-Barrera, R. Pérez-Hernández, Hydrogen production from oxidative steam reforming of methanol: Effect of the Cu and Ni impregnation on ZrO2 and their molecular simulation studies, International Journal of Hydrogen Energy, 37 (2012) 9018-9027.

[15] P. Mierczynski, A. Mierczynska, W. Maniukiewicz, T.P. Maniecki, K. Vasilev, MWCNTs as a catalyst in oxy-steam reforming of methanol, RSC Advances, 6 (2016) 81408-81413.

[16] C.-C. Chang, C.-T. Chang, S.-J. Chiang, B.-J. Liaw, Y.-Z. Chen, Oxidative steam reforming of methanol over CuO/ZnO/CeO2/ZrO2/Al2O3 catalysts, International Journal of Hydrogen Energy, 35 (2010) 7675-7683.

[17] C.-C. Chang, C.-C. Hsu, C.-T. Chang, Y.-P. Chen, B.-J. Liaw, Y.-Z. Chen, Effect of noble metal on oxidative steam reforming of methanol over CuO/ZnO/Al2O3 catalysts, International Journal of Hydrogen Energy, 37 (2012) 11176-11184.

[18] R. Pérez-Hernández, A. Gutiérrez-Martínez, C.E. Gutiérrez-Wing, Effect of Cu loading on for hydrogen production by oxidative steam reforming of methanol, International Journal of Hydrogen Energy, 32 (2007) 2888-2894.

[19] S. Sá, H. Silva, L. Brandão, J.M. Sousa, A. Mendes, Catalysts for methanol steam reforming—A review, Applied Catalysis B: Environmental, 99 (2010) 43-57.

[20] R. Pérez-Hernández, A. Gutiérrez-Martínez, M.E. Espinosa-Pesqueira, M.L. Estanislao, J. Palacios, Effect of the bimetallic Ni/Cu loading on the ZrO2 support for H2 production in the autothermal steam reforming of methanol, Catalysis Today, 250 (2015) 166-172.

[21] S.T. Yong, C.W. Ooi, S.P. Chai, X.S. Wu, Review of methanol reforming-Cu-based catalysts, surface reaction mechanisms, and reaction schemes, International Journal of Hydrogen Energy, 38 (2013) 9541-9552.

[22] R. Pérez-Hernández, G. Mondragón Galicia, D. Mendoza Anaya, J. Palacios, C. Angeles-Chavez, J. Arenas-Alatorre, Synthesis and characterization of bimetallic Cu–Ni/ZrO2 nanocatalysts: H2 production by oxidative steam reforming of methanol, International Journal of Hydrogen Energy, 33 (2008) 4569-4576.

[23] H.-M. Yang, M.-K. Chan, Steam reforming of methanol over copper–yttria catalyst supported on praseodymium–aluminum mixed oxides, Catalysis Communications, 12 (2011) 1389-1395.

[24] R. Perez-Hernandez, G. Mondragon-Galicia, A. Allende Maravilla, J. Palacios, Nano-dimensional CeO2 nanorods for high Ni loading catalysts: H2 production by autothermal steam reforming of methanol reaction, Physical Chemistry Chemical Physics, 15 (2013) 12702-12708.

[25] M. Turco, G. Bagnasco, C. Cammarano, P. Senese, U. Costantino, M. Sisani, Cu/ZnO/Al2O3 catalysts for oxidative steam reforming of methanol: The role of Cu and the dispersing oxide matrix, Applied Catalysis B: Environmental, 77 (2007) 46-57.

[26] C. Pojanavaraphan, U. Satitthai, A. Luengnaruemitchai, E. Gulari, Activity and stability of Au/CeO2–Fe2O3 catalysts for the hydrogen production via oxidative steam reforming of methanol, Journal of Industrial and Engineering Chemistry, 22 (2015) 41-52.

[27] M. Turco, G. Bagnasco, U. Costantino, F. Marmottini, T. Montanari, G. Ramis, G. Busca, Production of hydrogen from oxidative steam reforming of methanol: I. Preparation and characterization of Cu/ZnO/Al2O3 catalysts from a hydrotalcite-like LDH precursor, Journal of Catalysis, 228 (2004) 43-55.

[28] C. Pojanavaraphan, A. Luengnaruemitchai, E. Gulari, Catalytic activity of Au-Cu/CeO2-ZrO2 catalysts in steam reforming of methanol, Applied Catalysis A: General, 456 (2013) 135-143.

[29] L. Yong-Feng, D. Xin-Fa, L. Wei-Ming, Effects of ZrO2-promoter on catalytic performance of CuZnAlO catalysts for production of hydrogen by steam reforming of methanol, International Journal of Hydrogen Energy, 29 (2004) 1617-1621.

[30] V. Dal Santo, A. Gallo, A. Naldoni, M. Guidotti, R. Psaro, Bimetallic heterogeneous catalysts for hydrogen production, Catalysis Today, 197 (2012) 190-205.

[31] S.J. Hassani Rad, M. Haghighi, A. Alizadeh Eslami, F. Rahmani, N. Rahemi, Sol–gel vs. impregnation preparation of MgO and CeO2 doped Ni/Al2O3 nanocatalysts used in dry reforming of methane: Effect of process conditions, synthesis method and support composition, International Journal of Hydrogen Energy, 41 (2016) 5335-5350.

[32] H. Li, H. Xu, J. Wang, Methane reforming with CO2 to syngas over CeO 2-promoted Ni/Al2O3-ZrO2 catalysts prepared via a direct sol-gel process, Journal of Natural Gas Chemistry, 20 (2011) 1-8.

[33] W. Ahmed, A.E. Awadallah, A.A. Aboul-Enein, Ni/CeO2–Al2O3 catalysts for methane thermo-catalytic decomposition to COx-free H2 production, International Journal of Hydrogen Energy, 41 (2016) 18484-18493.

Peer-reviewed version available at *Catalysts* **2018**, *8*, 380; doi:10.3390/catal8090380

[34] D. Das, J. Llorca, M. Dominguez, S. Colussi, A. Trovarelli, A. Gayen, Methanol steam reforming behavior of copper impregnated over CeO2–ZrO2 derived from a surfactant assisted coprecipitation route, International Journal of Hydrogen Energy, 40 (2015) 10463-10479.

[35] P. Mierczynski, R. Ciesielski, A. Kedziora, O. Shtyka, T.P. Maniecki, Methanol Synthesis Using Copper Catalysts Supported on CeO2−Al2O3 Mixed Oxide, Fibre Chemistry, (2017) 1-5.

[36] G. Li, L. Hu, J.M. Hill, Comparison of reducibility and stability of alumina-supported Ni catalysts prepared by impregnation and co-precipitation, Applied Catalysis A: General, 301 (2006) 16-24.

[37] R.-t. Guo, Y. Zhou, W.-g. Pan, J.-n. Hong, W.-l. Zhen, Q. Jin, C.-g. Ding, S.-y. Guo, Effect of preparation methods on the performance of CeO2/Al2O3 catalysts for selective catalytic reduction of NO with NH3, Journal of Industrial and Engineering Chemistry, 19 (2013) 2022-2025.

[38] M.-Y. Ding, J.-Y. Tu, T.-J. Wang, L.-L. Ma, C.-G. Wang, L.-G. Chen, Bio-syngas methanation towards synthetic natural gas (SNG) over highly active Al2O3–CeO2 supported Ni catalyst, Fuel Processing Technology, 134 (2015) 480-486.

[39] M.P. Kapoor, Y. Ichihashi, K. Kuraoka, W.-J. Shen, Y. Matsumura, Catalytic Methanol Decomposition Over Palladium Deposited on Mesoporous Cerium Oxide, Catalysis Letters, 88 (2003) 83-87.

[40] M.P. Kapoor, Y. Ichihashi, K. Kuraoka, Y. Matsumura, Catalytic methanol decomposition over palladium deposited on thermally stable mesoporous titanium oxide, Journal of Molecular Catalysis A: Chemical, 198 (2003) 303-308.

[41] M. Lenarda, E. Moretti, L. Storaro, P. Patrono, F. Pinzari, E. Rodríguez-Castellón, A. Jiménez-López, G. Busca, E. Finocchio, T. Montanari, R. Frattini, Finely dispersed Pd-Zn catalyst supported on an organized mesoporous alumina for hydrogen production by methanol steam reforming, Applied Catalysis A: General, 312 (2006) 220-228.

[42] Y.-H. Chin, R. Dagle, J. Hu, A.C. Dohnalkova, Y. Wang, Steam reforming of methanol over highly active Pd/ZnO catalyst, Catalysis Today, 77 (2002) 79-88.

[43] M.L. Cubeiro, J.L.G. Fierro, Selective Production of Hydrogen by Partial Oxidation of Methanol over ZnO-Supported Palladium Catalysts, Journal of Catalysis, 179 (1998) 150-162.

[44] J.M. Rynkowski, T. Paryjczak, A. Lewicki, M.I. Szynkowska, T.P. Maniecki, W.K. Jóźwiak, Characterization of Ru/CeO2-Al2O3 catalysts and their Performance in CO2 Methanation, Reaction Kinetics and Catalysis Letters, 71 (2000) 55-64.

[45] P. Mierczynski, W. Maniukiewicz, T. Maniecki, Comparative studies of Pd, Ru, Ni, Cu/ZnAl2O4 catalysts for the water gas shift reaction (vol 11, pg 912, 2013), Central European Journal of Chemistry, 11 (2013) 1255-1255.

[46] W. Zheng, J. Zhang, Q. Ge, H. Xu, W. Li, Effects of CeO2 addition on Ni/Al2O3 catalysts for the reaction of ammonia decomposition to hydrogen, Applied Catalysis B: Environmental, 80 (2008) 98-105.

[47] P. Mierczynski, W. Maniukiewicz, T. Maniecki, Comparative studies of Pd, Ru, Ni, Cu/ZnAl2O4 catalysts for the water gas shift reaction, Central European Journal of Chemistry, 11 (2013) 912-919.

[48] T. Maniecki, K. Bawolak-Olczak, P. Mierczynski, W. Maniukiewicz, W. Jozwiak, Effect of the chemical composition of (MgO)(x)(Al2O3)(y) support on the catalytic performance of Ni and Ni-Au catalysts for the partial oxidation of methane, Chemical Engineering Journal, 154 (2009) 142-148.

Peer-reviewed version available at *Catalysts* **2018**, *8*, 380; doi:10.3390/catal8090380

[49] T. Maniecki, A. Stadnichenko, W. Maniukiewicz, K. Bawolak, P. Mierczynski, A. Boronin, W. Jozwiak, An active phase transformation on surface of Ni-Au/Al2O3 catalyst during partial oxidation of methane to synthesis gas, Kinetics and Catalysis, 51 (2010) 573-578.

[50] M. Ding, J. Tu, Q. Zhang, M. Wang, N. Tsubaki, T. Wang, L. Ma, Enhancement of methanation of bio-syngas over CeO2-modified Ni/Al2O3 catalysts, Biomass and Bioenergy, 85 (2016) 12-17.

[51] H. Wu, G. Pantaleo, V. La Parola, A.M. Venezia, X. Collard, C. Aprile, L.F. Liotta, Bi- and trimetallic Ni catalysts over Al2O3 and Al2O3-MOx (M = Ce or Mg) oxides for methane dry reforming: Au and Pt additive effects, Applied Catalysis B: Environmental, 156–157 (2014) 350-361.

[52] P. Osorio-Vargas, N.A. Flores-González, R.M. Navarro, J.L.G. Fierro, C.H. Campos, P. Reyes, Improved stability of Ni/Al2O3 catalysts by effect of promoters (La2O3, CeO2) for ethanol steam-reforming reaction, Catalysis Today, 259, Part 1 (2016) 27-38.

[53] B.M. Reddy, K.N. Rao, G.K. Reddy, A. Khan, S.-E. Park, Structural Characterization and Oxidehydrogenation Activity of CeO2/Al2O3 and V2O5/CeO2/Al2O3 Catalysts, The Journal of Physical Chemistry C, 111 (2007) 18751-18758.

[54] Y. Jiao, J. Zhang, Y. Du, F. Li, C. Li, J. Lu, J. Wang, Y. Chen, Hydrogen production by catalytic steam reforming of hydrocarbon fuels over Ni/Ce–Al2O3 bifunctional catalysts: Effects of SrO addition, International Journal of Hydrogen Energy, 41 (2016) 13436-13447.

[55] I. Luisetto, S. Tuti, C. Battocchio, S. Lo Mastro, A. Sodo, Ni/CeO2–Al2O3 catalysts for the dry reforming of methane: The effect of CeAlO3 content and nickel crystallite size on catalytic activity and coke resistance, Applied Catalysis A: General, 500 (2015) 12-22.